nature chemical biology

Zinc pyrithione-mediated activation of voltage-gated KCNQ potassium channels rescues epileptogenic mutants

Qiaojie Xiong, Haiyan Sun & Min Li

KCNQ potassium channels are activated by changes in transmembrane voltage and play an important role in controlling electrical excitability. Human mutations of KCNQ2 and KCNQ3 potassium channel genes result in reduction or loss of channel activity and cause benign familial neonatal convulsions (BFNCs). Thus, small molecules capable of augmenting KCNQ currents are essential both for understanding the mechanism of channel activity and for developing therapeutics. We performed a high-throughput screen in search for agonistic compounds potentiating KCNQ potassium channels. Here we report identification of a new opener, zinc pyrithione (1), which activates both recombinant and native KCNQ M currents. Interactions with the channel protein cause an increase of single-channel open probability that could fully account for the overall conductance increase. Separate point mutations have been identified that either shift the concentration dependence or affect potentiation efficacy, thereby providing evidence for residues influencing ligand binding and downstream events. Furthermore, zinc pyrithione is capable of rescuing the mutant channels causal to BFNCs.

Voltage-gated potassium channels are important regulatory proteins for controlling electrical excitability[1,2]. One common feature of these proteins is the tight coupling of channel activity to transient changes in transmembrane potential[3]. Those channels with sensitivity to membrane potential changes near the resting potential have a critical role in controlling membrane excitability. One group of low-threshold non-inactivating potassium channels is characterized by potent inhibition upon activation of muscarinic receptors; hence, they are known as "M channels"[4,5]. Their biophysical properties together with specific protein subcellular localization enable powerful control of the firing rate of a neuron[6,7]. Because M channels are also inhibited by the neurotransmitter-activated G protein–coupled signaling pathway, the resultant downregulation of M current could also potentiate membrane excitability[8]. These opposing regulatory mechanisms are an important aspect of M-current physiology[5,9,10].

Molecular cloning and recombinant expression have identified five genes encoding KCNQ subunits 1–5 (also known as Kv7.1, Kv7.2, Kv7.3, Kv7.4 and Kv7.5)[11–16]. With the exception of KCNQ1, which is predominantly found in the cardiac system, the remaining four isoforms are neuronal. The heteromultimeric channels of KCNQ2 to KCNQ5 (especially KCNQ2 and KCNQ3) have biophysical and pharmacological properties reminiscent of those of the M channels[13,14,17,18]. Therefore, KCNQ potassium channels are important regulatory proteins for controlling electrical excitability[9,10,19].

Chemical modulators for ion channels are important tools for investigating ion channel properties—a notion exemplified by earlier work using the pore blocker tetraethylammonium (TEA; 2) to probe potassium channels[20–23]. Clinically, potassium channel blockers are known for both their broad utilities and side effects[24]. Indeed, certain potassium channels, especially hERG, seem to be 'magnets' for small-molecule drugs, which most commonly cause inhibition of hERG activity. Because of its critical importance in repolarization after cardiac action potentials, inhibition of hERG results in a longer QT interval, a common condition underlying cardiac side effects for a variety of drugs[25]. However, reversible activators for voltage-gated cation channels remain extremely rare and much harder to identify. Retigabine (3), (*N*-(2-amino-4-(4-fluorobenzylamino)-phenyl) carbamic acid ethyl ester), was first identified for its suspected agonistic effect on the GABAergic pathway[26,27]. Later it was found that potentiation of KCNQ M current seems to be responsible for its anticonvulsion activity[28,29]. More recently, sphingomyelinase activity from spider venom was found to irreversibly activate Kv2.1 channel activity, presumably through enzymatic modification of lipid molecules[30]. These agonists (despite the fact that few are currently available) promise to provide new insights into various aspects of channel function that are difficult to assess by other means.

To apply a chemical biology approach for systematic identification and evaluation of potassium channel modulators, we have developed a compound selection procedure for potassium channels by combining specific chemical bleaching of surfaced channels and time-course measurement of activity recovery by nonradioactive rubidium flux assays[31]. This technique has been tested for identification of inhibitors for Kir2.1 and hERG potassium channels with mechanisms of action that are either acute (via inhibition of channel activity) or chronic (via regulation of trafficking and/or half-life of channel proteins)[32]. Applying a similar strategy, we have set out to look for compounds with agonistic activities for KCNQ channels by screening large compound libraries. Here we report that zinc pyrithione (ZnPy) is an unusual

Department of Neuroscience, High Throughput Biology Center and Department of Physiology, School of Medicine, Johns Hopkins University, 733 North Broadway, Baltimore, Maryland 21205, USA. Correspondence should be addressed to M.L. (minli@jhmi.edu).

Received 7 December 2006; accepted 20 March 2007; published online 15 April 2007; doi:10.1038/nchembio874

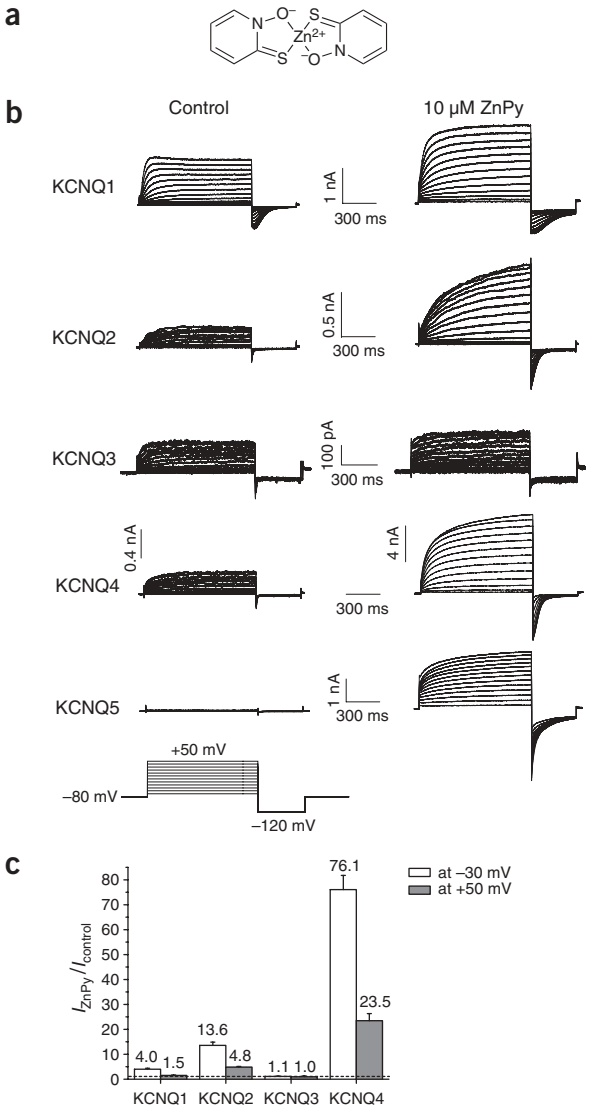

Figure 1 ZnPy potentiated potassium currents induced by KCNQ homomultimers. (**a**) Structure of ZnPy according to crystallographic studies. (**b**) Whole-cell currents of CHO cells transfected individually with KCNQ1 to KCNQ5 were recorded in the absence (left panels) and presence (right panels) of 10 μM ZnPy. Holding potential (V_h) was –80 mV, in 10 mV incremental voltage steps from –70 mV to +50 mV (insert). Scale bars are as indicated. (**c**) Histogram plotting the ZnPy effect on KCNQ currents at both –30 mV (open box) and +50 mV (filled box). The current amplitude is shown as normalized current ($I_{ZnPy}/I_{control}$). The number of folds of current increase is indicated above each column ($n \geq 4$). The dashed line indicates the potentiation of 1 ($I_{ZnPy}/I_{control} = 1$)—that is, no effect. Data are presented as means ± s.e.m.

synthetic potentiator that potently activates both heterologous and native M channels by inducing channel opening at the resting potential. Furthermore, it is capable of chemical rescue of certain genetic mutations found in people who suffer from neonatal epilepsy and myokymia.

RESULTS

Isolation of KCNQ channel modulators

To identify compounds with agonistic activities for M currents, we have generated stable cell lines for both KCNQ2 and KCNQ2/3. Under a precalibrated condition of medium-level rubidium efflux responses, we screened more than 20,000 small-molecule compounds at a concentration of 10 μM (see Methods)[32]. The selected condition allows for identification of both inhibitors and potentiators. We have identified 270 potentiators and 409 inhibitors, which either increase or decrease the rubidium responses by more than 15% when compared to the control. A subset of the compounds has been selected and validated for both potency and specificity. Among them, ZnPy showed unusual potency in elevating KCNQ activities, as judged by the nonradioactive rubidium efflux assay[31,33] (**Fig. 1a**).

Protein sequences of KCNQ1 to KCNQ5 share considerable sequence homology. To determine target specificity of ZnPy, we individually expressed and then tested KCNQ1 to KCNQ5 in Chinese hamster ovary (CHO) cells for their sensitivity to ZnPy using a whole-cell voltage-clamp technique. Except for KCNQ3, the activities of all KCNQ subtypes were potentiated by extracellular treatment with 10 μM ZnPy (**Fig. 1b**). KCNQ5 had little or no current under the expression condition used in the current studies. Surprisingly, ample KCNQ5 proteins were present on the cell surface and became conductive upon ZnPy treatment. The observed potentiation was rapidly reversible and was not accompanied by any significant changes in membrane capacitance. Thus, regulation of channel density by trafficking could not be the primary mechanism responsible for the potentiation. Depending on the specific channel, we observed a 4- to 76-fold increase at –30 mV and a 1.5- to 24-fold increase at +50 mV ($n \geq 4$, $P < 0.001$) (**Fig. 1c**). The effects on KCNQ5 were reproducible but not included in **Figure 1c**, because the KCNQ5-specific current in the absence of ZnPy could not be reliably determined. In additional tests of other channels, we found that ZnPy does not potentiate channel activities of hERG, Kv2.1 delay rectifier voltage-gated potassium channel, Kv4.2 A-type potassium channel or N-type calcium channel (**Supplementary Fig. 1** online). These results are evidence for target-specific potentiation.

To be more certain that the effects were exerted on potassium conductance, we examined the current sensitivity to TEA, a common inhibitor for potassium channels. KCNQ2 currents were completely blocked by 20 mM external TEA, consistent with earlier reports (**Fig. 2a**)[17,18]. Extracellular application of 10 μM ZnPy did not reverse the TEA inhibition. However, the removal of TEA allowed for immediate recovery of ionic current and a continuation of potentiation above the initial amplitude, presumably by ZnPy. Indeed, subsequent removal of ZnPy reversed the current to the initial amplitude (**Fig. 2a**). Linopirdine (4) inhibits both native M currents and

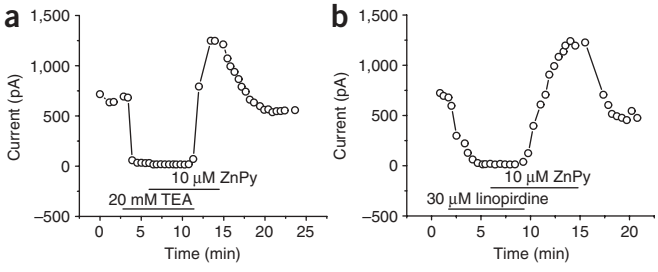

Figure 2 Combinatorial effects on KCNQ2 current by potassium channel blockers and ZnPy. Representative time course recordings of KCNQ2 current at +50 mV are shown. (**a**,**b**) The time periods of external application of 20 mM TEA (**a**) or 30 μM linopirdine (**b**) and overlapping applications of ZnPy are as shown ($n \geq 4$).

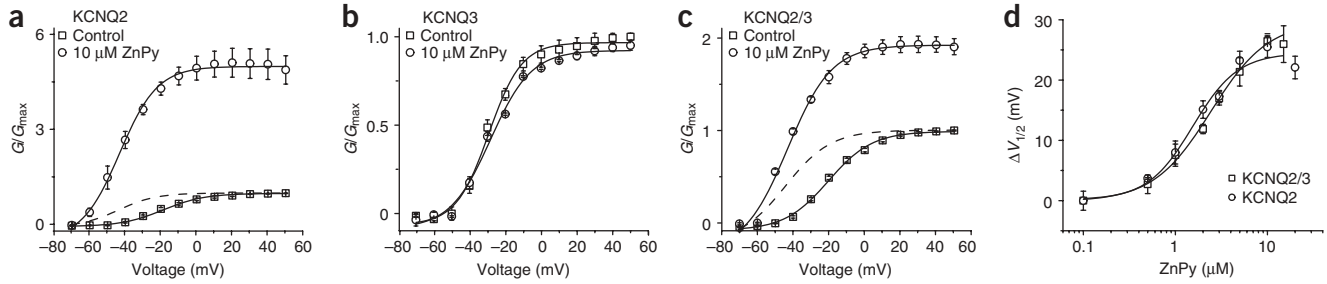

Figure 3 Biophysical effects of ZnPy on KCNQ channels. (**a**) G-V curves of KCNQ2 homomultimers. (**b**,**c**) KCNQ3 homomers (**b**) and KCNQ2/3 heteromers (**c**) in the absence (square) or presence (circle) of 10 μM ZnPy ($n \geq 4$, $P < 0.001$). Conductance at each depolarized voltage (from −70 mV to +50 mV) was normalized to the conductance at +50 mV (G_{max}) in the absence of ZnPy. Dashed lines are fit curves for KCNQ2 (**a**) and KCNQ2/3 (**c**) in the presence of ZnPy after recalling the G_{max} to 1. (**d**) Midpoint of activation voltage shifts of KCNQ2 (circle) and KCNQ2/3 (square) induced by ZnPy at different concentrations ($n \geq 4$). Curves shown are the fit of concentration-response curves to the mean values, with EC_{50} of 1.5 μM for KCNQ2 alone and 2.4 μM for KCNQ2/3 heteromultimers. Data are presented as means ± s.e.m.

recombinantly expressed KCNQ channels[34]. Indeed, 30 μM linopirdine caused a rapid inhibition of KCNQ2 current in CHO cells. Similar to the TEA treatment above, continued perfusion of ZnPy induced a substantial potentiation after removal of linopirdine (**Fig. 2b**). Thus, ZnPy acts on KCNQ-induced potassium current.

To determine whether Zn^{2+} and/or pyrithione are the causal factors for the potentiation, we tested their effects using a CHO cell line expressing KCNQ2 by whole-cell voltage clamp. Sodium pyrithione (NaPy; 5) is water soluble and ionizes at pH 7.8. No change in current amplitude was observed at 20 μM sodium pyrithione. Supplementation of 10 μM $ZnSO_4$ to the perfusion, which allows for the formation of ZnPy, induced a marked increase in current amplitude (**Supplementary Fig. 2** online). The potentiation was abolished by 4-(2)-(pyridylazo)resorcinol (PAR; 6), a potent zinc chelator. PAR itself had no effect on KCNQ2 channel activity. Furthermore, substitution of $ZnSO_4$ with $CuSO_4$ or $CdCl_2$ in the above experiments did not induce any potentiation (**Supplementary Fig. 3** online). Hence, zinc and ionized pyrithione, either as a mixture of two independent entities or in a complexed form, are sufficient in conferring potentiation. To determine whether the two chemical components, zinc and pyrithione, might function independently but in a mixture, we took advantage of the fact that the formation of ZnPy from zinc salts and non-ionized pyrithione requires incubation at 90 °C under alkaline conditions[35,36] (**Supplementary Fig. 4** online). Such a mixture without a prior incubation at 90 °C had no effect on the current amplitude (**Supplementary Fig. 2**). These results, combined with the stoichiometric requirements below (**Supplementary Fig. 5** online), support the notion that ZnPy as a complexed form is likely to be causal to the potentiation. The data, however, cannot formally rule out that Zn^{2+} and ionized pyrithione, as two separate components, work in concert to contribute the augmentation.

ZnPy is an ionophore[37]. To distinguish potential chemical interaction with the channel proteins from ionophore effects, we tested for any modulatory effects by three additional zinc ionophores: zinc diethyldithiocarbamate (DEDTC; 7), 5,7-diiodo-8-hydroxyquinoline (DIQ; 8) and (±)-α-tocopherol (VE; 9). None had any potentiation effect on current amplitude (**Supplementary Fig. 2**), which indicates that the ionophore effect alone is not sufficient for the observed potentiation.

ZnPy, if causal to the potentiation, should have a preferential stoichiometry. Based on crystallographic studies and elemental analyses[38], ZnPy is a complex of one zinc atom chelated by two pyrithione units by way of sulfur and oxygen atoms (**Supplementary Fig. 5**). Because organic solvents were used in these earlier studies, we sought to test the optimal stoichiometry for potentiation of KCNQ channels in aqueous solution. **Supplementary Figure 5** shows the effects of potentiation induced by different ratios of sodium pyrithione and $ZnSO_4$. At a constant combined final concentration of 30 μM, the maximal potentiation was observed at a 2:1 ratio mixture of sodium pyrithione to $ZnSO_4$. This ratio of mixture is chemically comparable to that of 10 μM ZnPy. Indeed, the degree of potentiation is substantial but slightly less than that of 10 μM preformed ZnPy (**Fig. 1c**). Together, these results are in agreement with the notion that the potentiation caused by interaction with the KCNQ channel protein is dependent on specific stoichiometry of ZnPy.

Mechanistic characterization of ZnPy modulation

To study mechanisms for the potentiation, voltage-dependent activation was examined using heterologously expressed KCNQ2 and KCNQ3 channels. In the presence of 10 μM ZnPy, the $V_{1/2}$ (voltage required for half-maximal activation) of KCNQ2 was left-shifted by as much as 25.5 ± 1.5 mV (mean ± s.e.m.), from −18.9 ± 0.6 mV to −44.4 ± 0.9 mV ($n \geq 4$, $P < 0.001$). In contrast, KCNQ3, which did not show any current potentiation by ZnPy (**Fig. 1b**), also showed no change in $V_{1/2}$ (**Fig. 3a**,**b**). Heteromultimeric assembly of KCNQ2 and KCNQ3 channels is thought to be the molecular constituent for M current. ZnPy consistently caused a hyperpolarizing shift of $V_{1/2}$ of KCNQ2/3 channels by 24.4 ± 0.8 mV, from −20.3 ± 0.8 mV to −44.7 ± 1.9 mV ($n \geq 4$, $P < 0.001$) (**Fig. 3c**). The effect of ZnPy was dose-dependent and had an EC_{50} value of 1.5 ± 0.3 μM for KCNQ2 and 2.4 ± 0.4 μM for KCNQ2/3 (**Fig. 3d**). This supports a 'dominant' role for KCNQ2 in conferring sensitivity to ZnPy. The dosage-dependent curve was fitted with a Hill equation with a coefficient of 1.8 for KCNQ2 and 1.4 for KCNQ2/3.

In addition to the hyperpolarizing shift of $V_{1/2}$, ZnPy markedly reduced both activation and deactivation rates. Specifically, the activation time constant of KCNQ2/3 at +50 mV changed from 75.6 ± 4.9 to 157.8 ± 23.5 ms ($n = 6$, $P < 0.001$), and it changed similarly from 163.5 ± 13.7 to 293.1 ± 11.2 ms ($n = 5$, $P < 0.001$) for KCNQ2. The deactivation time constant for KCNQ2/3 at −120 mV increased from 12.4 ± 0.7 to 41.9 ± 6.4 ms ($n = 8$, $P < 0.001$), and from 14.1 ± 0.6 to 54.4 ± 0.9 ms ($n = 4$, $P < 0.001$) for KCNQ2 (**Supplementary Fig. 6** online). The combination of increase of maximal conductance (G_{max}) and hyperpolarizing shift of half-maximal activation contributes to the overall augmentation of current amplitude.

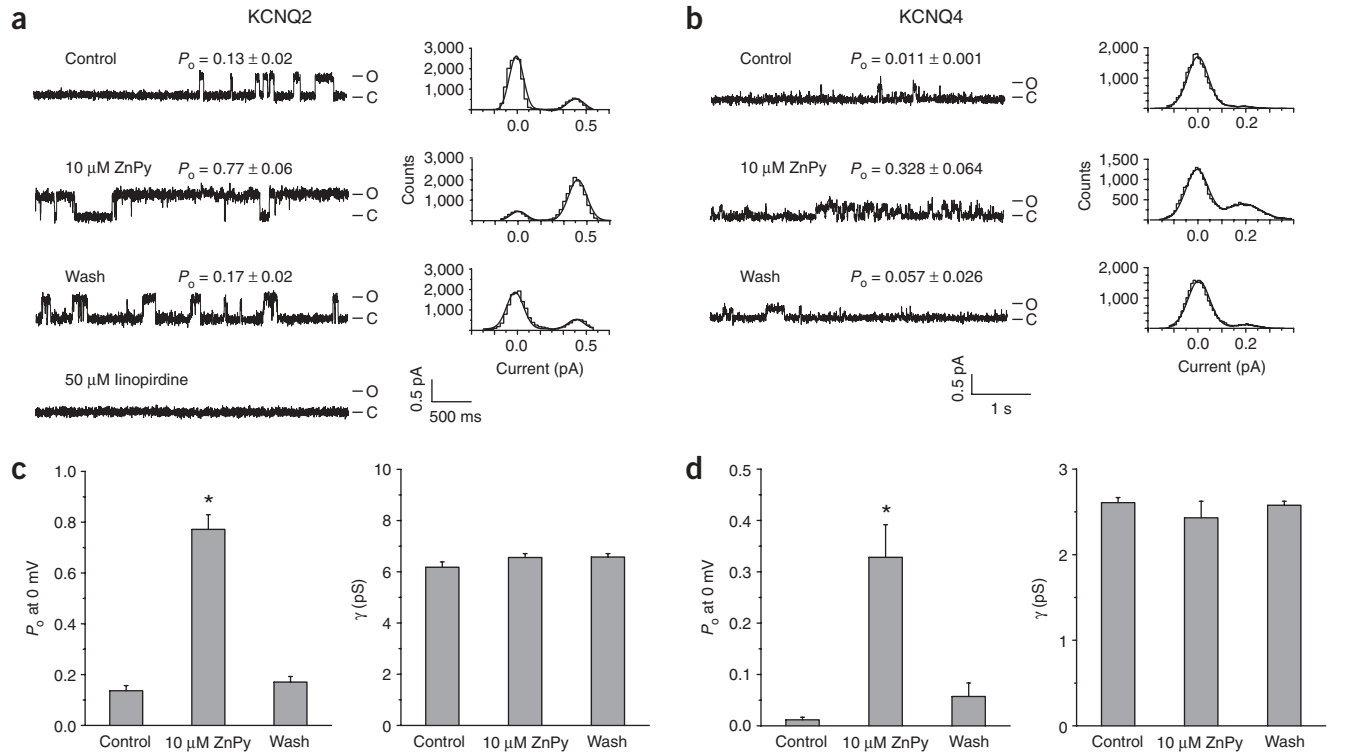

Figure 4 ZnPy increases the P_o of KCNQ2 channel. (**a**) Single-channel signals from outside-out patches clamped at 0 mV in the absence and presence of 10 μM ZnPy, or 50 μM linopirdine (left panel). All-point amplitude histograms for the sweeps shown on the left (right panel). The fitted unitary current amplitudes and P_o at 0 mV were: 0.51 pA and 0.13 (control), 0.52 pA and 0.77 (ZnPy), and 0.52 pA and 0.17 (wash). O, open; C, close. (**b**) KCNQ4 single-channel signals from outside-out patches clamped at 0 mV in the absence and presence of 10 μM ZnPy (left panel). All-point amplitude histograms for the sweeps shown on the left (right panel). The fitted unitary current amplitudes and P_o at 0 mV were: 0.20 pA and 0.011 (control), 0.19 pA and 0.328 (ZnPy), and 0.20 pA and 0.057 (wash). (**c**) Histograms show the P_o values at 0 mV in the absence and presence of ZnPy ($n = 5$, $^*P < 0.001$) (left panel). Histograms show the single-channel conductance (γ) in the absence and presence of ZnPy ($n = 5$) (right panel). (**d**) Histograms show the KCNQ4 P_o values at 0 mV in the absence and presence of ZnPy ($n = 4$, $^*P < 0.001$) (left panel). Histograms show the single-channel conductance (γ) in the absence and presence of ZnPy ($n = 4$) (right panel). Data are presented as means ± s.e.m.

To be more certain about the mechanism of G_{max} augmentation by ZnPy, we recorded single-channel activities of KCNQ2 and KCNQ4 at 0 mV saturated voltage (**Fig. 4**). We observed a significant increase of single-channel open probability (P_o) for KCNQ2, from 0.13 ± 0.02 to 0.77 ± 0.06 ($n = 5$, $P < 0.001$) in the presence of 10 μM ZnPy (**Fig. 4a**). The single-channel activity was fully blocked by linopirdine. Consistent with macroscopic measurements, the ZnPy effects were fully reversible (**Fig. 4c**) and showed single-channel conductance of 6.6 ± 0.15 pS ($n = 5$) in the presence or absence of ZnPy (**Fig. 4b**). The 5.9-fold increase in P_o in the presence of 10 μM ZnPy could fully account for the overall augmentation of G_{max}. Similarly, ZnPy increased the P_o of KCNQ4 from 0.011 ± 0.001 to 0.328 ± 0.064 ($n = 4$, $P < 0.001$). The single-channel conductance of 2.4 ± 0.1 pS ($n = 4$) remained consistent and the effects were largely reversible. Consistent with that of KCNQ2, the increase in P_o could fully account for the augmentation of G_{max}. Hence, these data provided the evidence that the increase in P_o is a major contributing factor for the G_{max}.

Distinct interaction site of ZnPy

The effect of ZnPy was consistently observed by external application. To determine whether the effect could be achieved through intracellular application, we recorded KCNQ current using a pipette solution lacking EGTA but supplemented with 10 μM of ZnPy (**Supplementary Fig. 7** online). The channel activities were monitored over periods of more than 10 min, a condition previously confirmed to be sufficient for intracellular diffusion. ZnPy, when applied intracellularly, induced no potentiation, either with or without EGTA, which chelates Zn^{2+}. Under this condition, when ZnPy was applied externally, the potentiation was fully inducible (**Supplementary Fig. 7**). Because the current amplitude varies from cell to cell, to be more definitive, we chose to determine $V_{1/2}$ values at different times after establishing a stable seal and internal perfusion of ZnPy through a recording pipette. Indeed, the $V_{1/2}$ was consistent and identical to that of KCNQ2 control (**Supplementary Fig. 7**). This provides the evidence for external accessibility of ZnPy for KCNQ interactions.

Retigabine (RTG) binding to KCNQ channels causes $V_{1/2}$ shift to a more hyperpolarizing potential, with little change in overall conductance[29,34,39]. In addition, it is most effective on KCNQ3 and essentially has no effect on KCNQ1. These features represent an important distinction between retigabine and ZnPy. The KCNQ2 (W236L) mutant is a channel that is fully functional but no longer sensitive to RTG[40,41]. When treated with ZnPy, this mutant has sensitivity comparable to that of wild-type KCNQ2 at either –30 mV or +50 mV (**Supplementary Fig. 7**). Together, these observations suggest that ZnPy acts on a new site in causing its agonistic effects.

Alteration of $V_{1/2}$ and maximal conductance is consistent with a role of ZnPy interacting with the gating machinery. ZnPy seems to

access from the extracellular side, and many key residues of gating machinery lie between the S5 and S6 domains. To investigate the molecular determinants responsible for ZnPy effects, we constructed a series of site-directed mutants by systematically substituting residues with alanine covering and flanking the pore region (**Fig. 5**). **Figure 5a** shows those KCNQ2 mutants that are functional and their levels of sensitivity to ZnPy, displayed by number of folds of current increase at +50 mV induced. Examining both $V_{1/2}$ and folds of increase revealed several positions contributing to ZnPy sensitivity. Of particular significance, several mutants (such as L249A and L275A) showed robust functional channels but with reduced changes in $V_{1/2}$ when compared to that of the wild type. We thus hypothesize that double mutation of

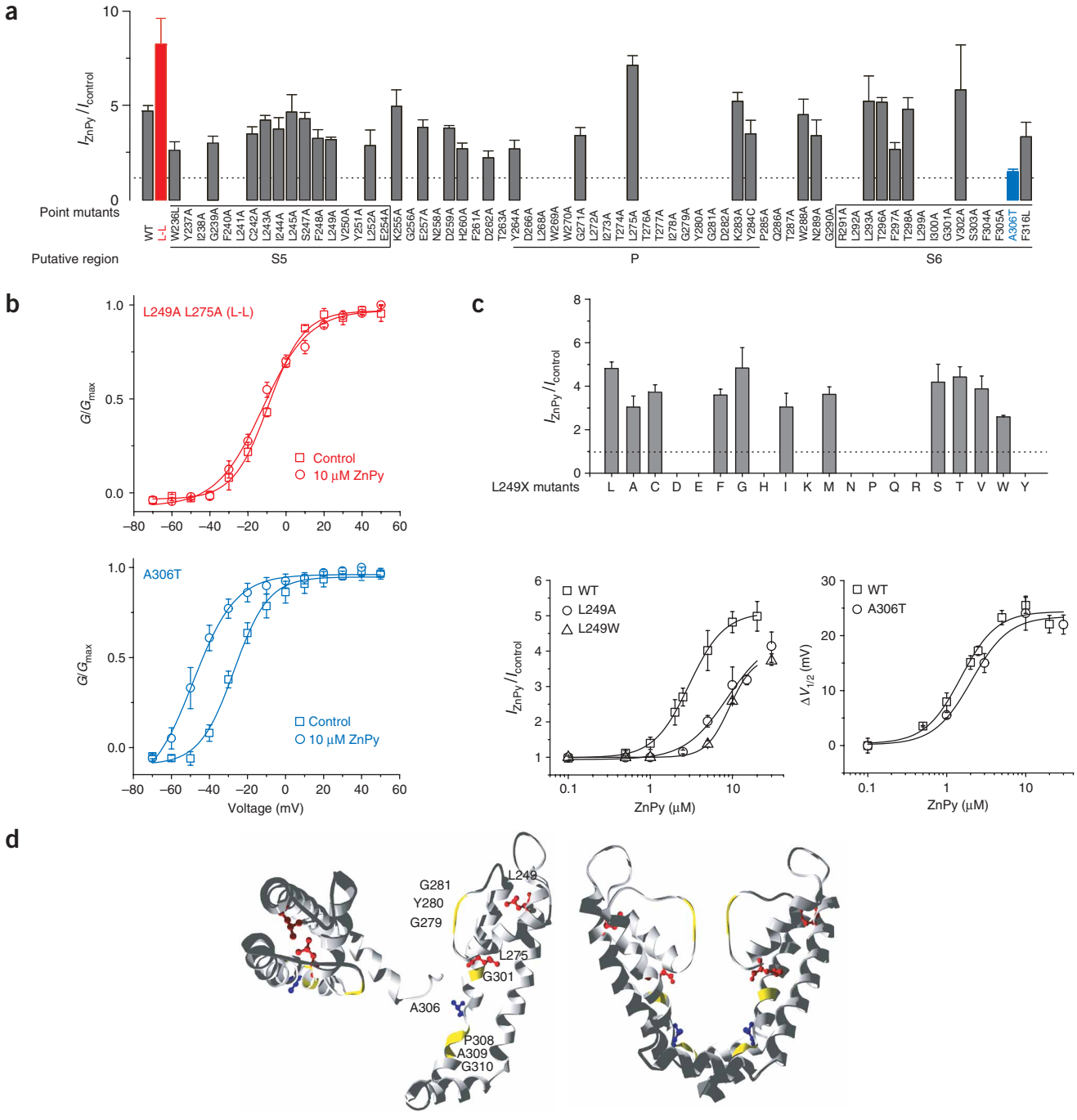

Figure 5 Molecular determinants for ZnPy sensitivity. (**a**) Histogram shows the current (+50 mV) potentiation effect of ZnPy on KCNQ2 S5-S6 point mutants ($n \geq 3$). Each mutation site was indicated based on the predicted transmembrane regions. Dashed line indicates a potentiation level of 1 (that is, no effect). (**b**) Activation curves of KCNQ2 (L249A L275A) (red) in the presence and absence of ZnPy ($n \geq 4$, $P > 0.1$) (top). Activation curves of KCNQ2 (A306T) (blue) in the presence and absence of ZnPy (bottom). (**c**) Histogram shows the current (+50 mV) potentiation effect of ZnPy on KCNQ2 (L249X) mutants ($n \geq 3$) (top). Dose-response curves of wild-type (WT) KCNQ2, L249A and L249W for ZnPy, with EC_{50} of 2.9 ± 0.1, 8.6 ± 1.7 and 9.2 ± 0.1 μM, respectively (bottom left). Dose-response curves of wild-type KCNQ2 and A306T for ZnPy, with EC_{50} of 1.5 ± 0.2 and 2.1 ± 0.5 μM, respectively (bottom right). (**d**) Modeling of the S5-pore-S6 region of KCNQ2. The key residues are as highlighted. Data are presented as means ± s.e.m.

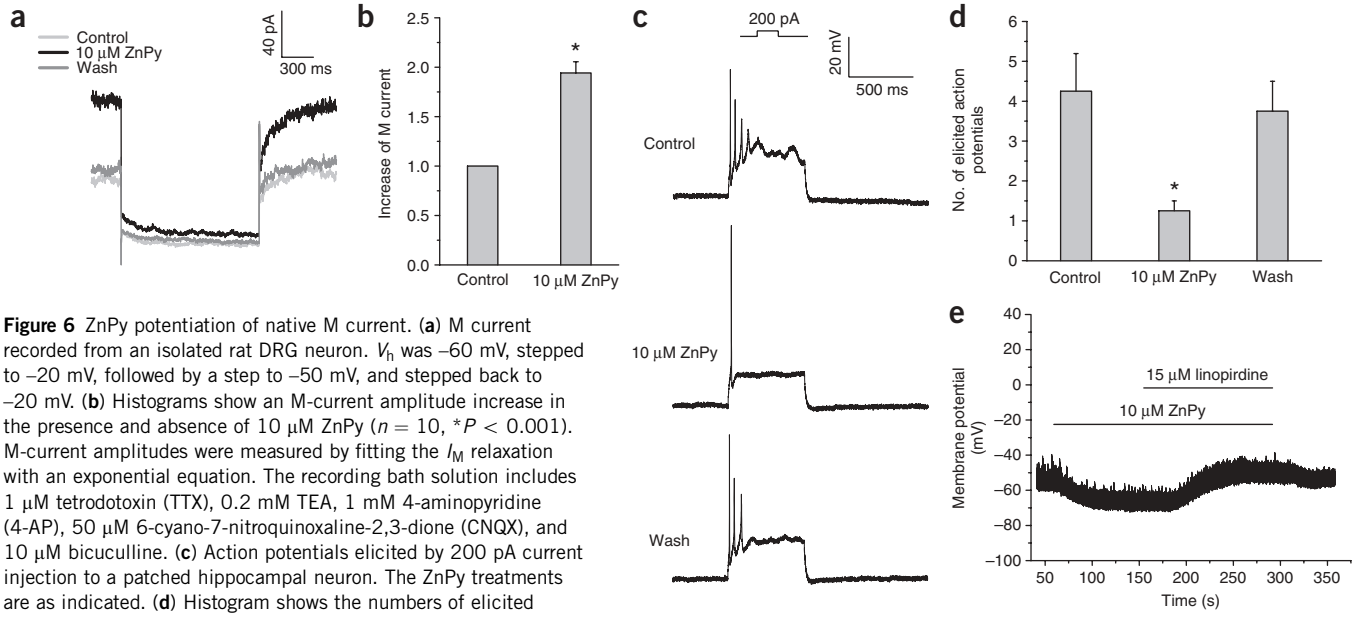

Figure 6 ZnPy potentiation of native M current. (**a**) M current recorded from an isolated rat DRG neuron. V_h was –60 mV, stepped to –20 mV, followed by a step to –50 mV, and stepped back to –20 mV. (**b**) Histograms show an M-current amplitude increase in the presence and absence of 10 μM ZnPy ($n = 10$, $^*P < 0.001$). M-current amplitudes were measured by fitting the I_M relaxation with an exponential equation. The recording bath solution includes 1 μM tetrodotoxin (TTX), 0.2 mM TEA, 1 mM 4-aminopyridine (4-AP), 50 μM 6-cyano-7-nitroquinoxaline-2,3-dione (CNQX), and 10 μM bicuculline. (**c**) Action potentials elicited by 200 pA current injection to a patched hippocampal neuron. The ZnPy treatments are as indicated. (**d**) Histogram shows the numbers of elicited action potentials before and after 10 μM ZnPy application ($n = 4$, $^*P < 0.001$). (**e**) Membrane potential of an isolated hippocampal neuron was monitored when 10 μM ZnPy was applied in bath solution followed by the addition of 15 μM linopirdine. Membrane potentials were 54.7 ± 0.6 mV (control) and 63.5 ± 1.3 mV (ZnPy) ($n = 4$, $P < 0.001$). Data are presented as means ± s.e.m.

these positions could potentially lead to complete loss of $V_{1/2}$ change. Unlike other double mutants, the double mutation of KCNQ2 (L249A L275A) was functional. Furthermore, it completely abolished the $V_{1/2}$ shift caused by ZnPy while displaying 8.6 ± 2.2 ($n = 3$, $P < 0.001$) folds of current increase (**Fig. 5a**,**b**). In contrast, KCNQ2 (A306T) showed little potentiation in G_{max} by ZnPy but remained sensitive to ZnPy, displaying the hyperpolarizing shift by 24.1 ± 3.1 mV ($n = 6$, $P < 0.001$) (**Fig. 5b**). Together, evidence from investigating these mutants begins to define molecular determinants critical for the ZnPy effects.

Using homology modeling and the published Kv1.2 structure[42], we assigned the locations of these three residues (**Fig. 5d**). The Leu249 and Leu275 residues face each other from two separate helices, which is consistent with a coordinated role. In contrast, the Ala306 residue is located deep in the structure between the proposed gating hinge and the bending region[43] (**Fig. 5d**; also see Discussion). Because ZnPy accesses the channel from the extracellular side (**Supplementary Fig. 7**), we speculate that the outer residue (Leu249) may influence binding by contributing either the formation of the binding site or pathway to the binding site, whereas the residues deep in the cytoplasmic side may influence the downstream effects upon binding. To test this hypothesis, we mutated Leu249 to all 19 other residues and determined that L249A and L249W have the most effects in reducing current potentiation under the same concentration (**Fig. 5c**). Examining the dose dependence of these two mutants revealed an EC_{50} shift from 2.9 ± 0.1 to 8.6 ± 1.7 and 9.2 ± 0.1 μM, respectively. In contrast, A306T has an EC_{50} value similar to that of the wild type (**Fig. 5c**). These experiments have provided evidence that is consistent with the idea that the Leu249 residue contributes to the ZnPy binding and/or affects the rate of ZnPy access to the binding site.

Potentiation of native M current by ZnPy

To examine any effect on native M current (**Fig. 6**), isolated neurons were recorded using a standard protocol. **Figure 6a** shows a typical M current recorded before and after addition of 10 μM ZnPy. Consistent with the level of current argumentation using heterologously expressed KCNQ2/3 channels (**Fig. 3c**), ZnPy induced a significant potentiation of 1.9-fold ($n = 10$, $P < 0.001$) (**Fig. 6b**). This provides further support that these neurons have M channels reminiscent of KCNQ2/3 heteromultimers. In CHO cells expressing the KCNQ2 channel, 10 μM ZnPy caused significant hyperpolarization (data not shown). Similarly, in hippocampal neurons, treatment with 10 μM ZnPy resulted in noticeable hyperpolarization of membrane potential (**Fig. 6e**). Application of an M-channel antagonist, linopirdine, completely abolished the hyperpolarization of membrane potential, which is consistent with the notion that ZnPy acts on M current. This result is also in agreement with earlier experiments in which ZnPy was unable to induce potentiation in the presence of linopirdine (**Fig. 2b**).

One of the primary physiological functions of M current is to suppress repetitive discharges in neurons. Persistence of repetitive firing by current injection was tested in the presence and absence of ZnPy. **Figure 6c** shows the induced action potential spikes fired by an isolated hippocampal neuron upon current injection. Perfusion of ZnPy immediately abolished the repetitive firing. The activity was restored after the removal of ZnPy (**Fig. 6c**, middle and lower panels; and **Fig. 6d**). Together, the above series of experiments provides direct evidence that ZnPy agonistically modulates native M current via a mechanism consistent with what has been characterized for recombinant KCNQ2/3 channels.

Rescue of mutant KCNQ channels

Mutations in genes encoding KCNQ2 and KCNQ3 have been found in people who suffer from BFNCs and myokymia[11,15,44]. The common phenotype of these mutants is reduction of KCNQ currents as a result of decrease in either channel activities or protein expression on the cell surface. Because BFNC is autosomal dominant, M currents in afflicted individuals will likely be heteromultimers of mutant and wild-type KCNQ2 and KCNQ3 subunits. ZnPy potently upregulates the KCNQ channels across a broad range of membrane potentials. We thus hypothesize that it could acutely potentiate channel activity of those

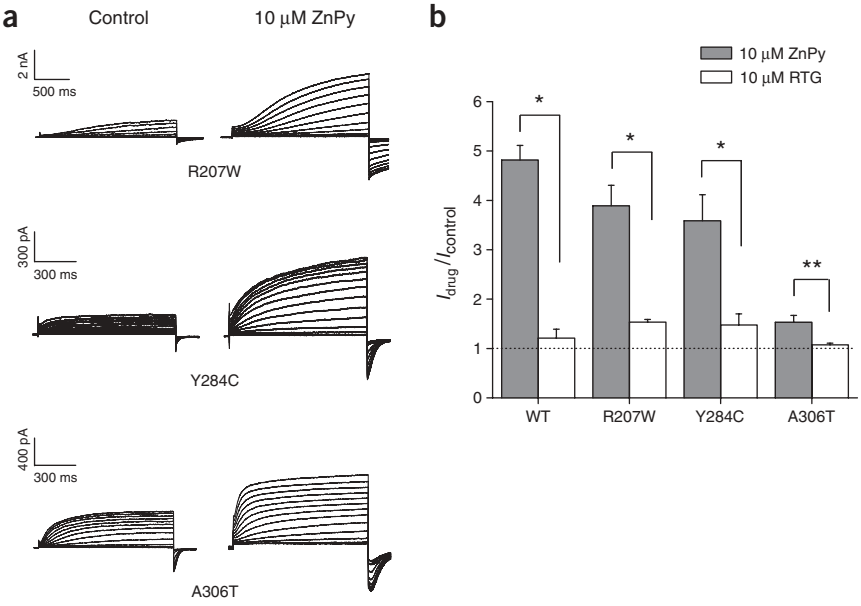

Figure 7 ZnPy effects on BFNC mutant channels expressed in CHO cells. (**a**) Whole-cell currents of KCNQ2 (R207W), KCNQ2 (Y284C) and KCNQ2 (A306T) were recorded in the absence (left) and presence (right) of 10 μM ZnPy. V_h was –80 mV, in 10 mV voltage steps from –70 mV to +50 mV. (**b**) Histogram plotting potentiation effects on KCNQ2 wild type and BFNC mutants (R207W, Y284C and A306T) by ZnPy (filled box) and retigabine (open box) ($n \geq 4$, $^*P < 0.001$, $^{**}P < 0.05$). Data are presented as means ± s.e.m.

mutants, thereby rescuing the channel activity. To test this notion, we chose to test homomultimers of KCNQ2, because ZnPy is dominant in conferring sensitivity (**Fig. 3c** and data not shown). We expressed three human mutations that have been previously shown to produce channel proteins with reduced conductivity: KCNQ2 (R207W), KCNQ2 (Y284C) and KCNQ2 (A306T)[15,45]. **Figure 7a** shows the current traces recorded from cells transiently transfected with each mutant. The increase caused by ZnPy was more than three-fold for both KCNQ2 (R207W) and KCNQ2 (Y284C) mutants ($n = 4$, $P < 0.001$). Consistently, ZnPy is less effective on KCNQ2 (A306T), which indicates that the integrity of this region is required for the ZnPy effect. In contrast, the same concentration of retigabine induced only modest potentiation for all mutants (**Fig. 7b**).

DISCUSSION

Ligand-mediated activation of KCNQ channels by ZnPy causes a significant hyperpolarization shift of voltage sensitivity and a marked reduction of the deactivation rate, resulting in channel opening across a wider range of membrane potential. Hence, in essence ZnPy effects confer a ligand-gating process in addition to voltage-gating for the KCNQ channels. The ZnPy-mediated opening may be observed under physiological resting potential (**Fig. 6**), resulting in hyperpolarization and causing KCNQ to function as a ligand-gated channel. These results provide experimental evidence that synthetic activators are capable of inducing activation of voltage-gated ion channels. ZnPy-induced opening is reminiscent of the Ca^{2+} effect on calcium-activated (BK) potassium channels, which are dually gated by membrane depolarization and intracellular Ca^{2+} concentrations. At high concentrations, Ca^{2+} can induce channel opening in the absence of membrane depolarization[46]. Similarly, transient receptor potential (TRP) channels (such as TRPM8) are sensitive to cold, menthol, voltage and PIP_2. Menthol binding induces a significant hyperpolarizing shift of $V_{1/2}$ from 32 to –31 mV (ref. 47).

Chemical openers for cation ion channels are very rare, especially considering the limited approaches available for identification. Using the reported approach and a nonradioactive rubidium efflux assay, we have optimized a screening condition capable of identifying both agonistic and antagonistic modulators of potassium channels[31]. Considering that agonistic activity is essentially a gain-of-function phenotype, the relatively large number of identified compounds with more than a 15% increase of Rb^+ efflux activity suggests a robust readout range for capturing compounds with agonistic activities. Because almost all potassium channels are permeable to rubidium and many have already been tested by rubidium flux assay using radioactive $^{86}Rb^+$, it is conceivable that the screening strategy reported here could be adapted to identify agonists for different potassium channels.

The structure of ZnPy is unique when compared with other identified structures, such as retigabine[28], that also show agonistic activity for KCNQ channels. The ability of ZnPy to activate the channel and to increase the overall conductance raises the question of whether ZnPy can affect KCNQ channels via multiple different mechanisms, including steady state expression on cell surface. Indeed, the KCNQ2 channel protein has a short half-life on the cell surface when compared to other potassium channels such as hERG (data not shown). ZnPy, like other identified compounds, could in principle act either chronically or acutely in potentiating channel activity. However, our evidence supports that the ZnPy effect on KCNQ2 and other KCNQ channels is mainly caused by an acute potentiation because of rapid and reversible effects in both heterologously expressed cells and cultured neurons (**Figs. 2** and **6**; **Supplementary Figs. 2** and **7**).

The single-channel conductance and open probability are consistent with those reported earlier[48]. One speculation is that the potentiation is primarily achieved by increasing open channel probability (P_o). Indeed, ZnPy potentiates four of five isoforms (KCNQ5 > KCNQ4 > KCNQ2 > KCNQ1) (**Fig. 1**). The increase in P_o for KCNQ2 and KCNQ4 at the saturation voltage could fully account for the overall increase of G_{max} (**Fig. 4**). The lack of any significant effect on KCNQ3 could be due to its near unity P_o (ref. 48). Our experiments with KCNQ3, however, have failed to show any $V_{1/2}$ shift or appreciable changes in other parameters by ZnPy. Hence, it remains unclear whether KCNQ3 interacts with ZnPy. The covalent modulation, for example by *N*-ethylmaleimide (NEM; **10**), was shown to act on the KCNQ channel from the intracellular side of the channel protein and has a different ranking order of efficacy, including effective potentiation, on KCNQ3 (ref. 48).

The reported evidence is consistent with a model of specific interaction between pyrithione and KCNQ channel proteins. One hypothesis is that the pyrithione has low affinity, but is markedly enhanced when it is complexed with a zinc ion. The specific 1:2 zinc-to-pyrithione stoichiometry shown in **Supplementary Figure 5** for the optimal potentiation raises the possibility that zinc has a chaperonic

role in 'dimerizing' pyrithione that is reminiscent of what has been observed for carbonic anhydrase II, in which zinc seems to have a role in mediating a specific but reversible interaction that is critical for holoenzyme function[49]. Indeed, a specific double mutant (R362H A419H) in the Shaker potassium channel showed a strong hyperpolarizing shift of the conductance-voltage (G-V) curve—an effect caused by Zn^{2+} binding[50]. However, the overall conductance of the Shaker potassium channel showed no change, which supports the idea that Zn^{2+} binding specifically stabilizes the activated state. The corresponding positions in the KCNQ2 channel are Arg198 and Lys255, which cannot interact with Zn^{2+} directly. In addition, Zn^{2+} alone cannot induce any detectable effect (**Supplementary Fig. 2**). This suggests that ZnPy confers the effects by a different molecular interaction.

ZnPy, in addition to having a higher potency than retigabine, seems to exert KCNQ potentiation by a different molecular mechanism. Most noticeably, ZnPy is fully effective in potentiating the KCNQ2 (W236L) mutant (**Supplementary Fig. 7**). However, this mutant is no longer sensitive to retigabine[40,41]. Furthermore, ZnPy potentiates KCNQ1 but has no effect on KCNQ3 (**Figs. 1** and **3**). In contrast, retigabine is most effective on KCNQ3 but does not affect KCNQ1. The effect of retigabine is mainly caused by a hyperpolarizing shift of voltage dependence. Hence, at saturated voltages such as +50 mV, retigabine induces minimal potentiation on BFNC mutant channels, whereas ZnPy exerts a potent effect via increase in G_{max} (**Fig. 7**).

With respect to the molecular determinants critical for the ZnPy effects, our data suggest that Leu249, Leu275 and Arg306 are important residues for conferring ZnPy sensitivity. Notably, the L249A L275A double mutant and the A306T mutant separately affect $V_{1/2}$ and G_{max} (**Fig. 5**). If one assumes that the structure of KCNQ2 is similar to that of Kv1.2 within the transmembrane pore region, Leu249 and Leu275 should be on two separate α-helices but facing the same side (**Fig. 5d**). The linear distance between these two residues is 10.6 Å, which would allow an interaction with ZnPy. If this is part of the binding site, the proximity to the selectivity filter could conceivably cause an increase in P_o. The concentration dependence for the Leu249 residue (**Fig. 5c**), though supportive of a role in influencing binding, also raises other questions, especially regarding why several other residues with smaller side chains are compatible but have little effect on overall conductance. The role of these residues in influencing $\Delta V_{1/2}$ is not clear given the wide range of changes of $\Delta V_{1/2}$ compared with that of the wild type in the absence of ZnPy. Because a parameter with sufficient deviation from wild type is necessary to evaluate whether different concentrations of ZnPy could overcome the deficit, and because a ZnPy concentration of 20 μM or higher is toxic (thereby preventing reliable recording of channel activity), future alternative approaches, such as photoaffinity labeling, may be more informative for identifying residues that form the ZnPy binding site.

Residue Arg306 is deeper inside the structure and positions between Gly301, the so-called gating hinge[42,51], and the conserved putative Pro-Ala-Gly bend of the S6 domain. Both are critical components for voltage-mediated gating in KCNQ channels[43]. Thus, these results indicate key residues required for ZnPy sensitivity. Their locations in channel structure are consistent with the notion that interaction with ZnPy causes stabilization of open conformation.

The potent effect of ZnPy in potentiating KCNQ channels both in heterologous expression systems and in neurons raises the possibility of its utility both as a chemical probe and as a possible lead for further development for potential therapeutic use. As a molecular probe, ZnPy is unique in its potency and mode of action. Because ZnPy potentiates KCNQ channels but not other voltage-gated potassium channels, it might be particularly useful for understanding the similarities and differences of these otherwise homologous potassium channels. ZnPy has been used widely for control of dandruff and treatment of psoriasis[52]. A recent report also suggests that it is neuroprotective[53]. Because zinc ions have complex roles in both normal neuronal function and pathology[54], further investigations are necessary to evaluate ZnPy in animal models and develop its derivatives for clinical use.

METHODS

Cell culture and transient transfection. CHO cells were grown in 50:50 DMEM/F12 (Cellgro) with 10% FBS (Gibco), 100 U ml^{-1} penicillin (Cellgro), 100 μg ml^{-1} streptomycin (Cellgro) and 2 mM L-glutamine (Gibco). At 24 h before transfection, cells were split and plated in 60-mm dishes and were transfected with Lipofectamine2000 reagent (Invitrogen) according to the manufacturer's instructions. At 24 h after transfection, cells were split and replated onto coverslips coated with poly-L-lysine (Sigma). Plasmid expressing $CD4^+$ complementary DNA as a marker was cotransfected with the channel cDNAs of human KCNQ1, human KCNQ4, rat KCNQ2, rat KCNQ3 and human KCNQ5. Before recording, anti-$CD4^+$ Dynabeads (Dynal Biotech Inc.) were added into the medium to allow for identification of the transfected cells. Stable lines expressing Kv2.1, hERG and Kv4.2 were generated by standard protocols using pcDNA3.1 and maintained in complete medium supplemented with 500 μg ml^{-1} G418.

KCNQ2 screen. Human embryonic kidney (HEK) 293 cells stably expressing rat KCNQ2 were resuspended in DMEM/F12 medium and plated at a density of 4×10^4 per well in 96-well plates coated with poly-L-lysine. Compound libraries used in this screen are Microsource Spectrum (http://www.msdiscovery.com/) and Chembridge DIVERSET (http://chembridge.com/). Cells were then incubated at 37 °C with 5% CO_2 overnight. 30 μl (per well) of DMEM/F12 medium containing 30 mM RbCl was added to the cells the next day, followed by incubation for an additional 3 h. Cell plating and reagent dispensing were performed using a Multidrop 384 dispenser (Thermo Electron Corporation).

Compound addition and Rb^+ efflux assays were programmed and performed on a Cybi-Well system (CyBio US Inc.) and a Tekbench liquid handling system (Tekcel Inc.), respectively. Briefly, 0.9 μl each of the 200× compound solution was added to 80 wells of each cell plate. To ensure assay reproducibility, 0.9 μl of 5% DMSO solution was added to each well in the first column of each cell plate along with the compound solutions; these wells were used as negative controls. Final DMSO concentration in the cell medium was kept at or below 0.1% for all cell plates to minimize any toxicity. After adding the compounds, the cells were again incubated at 37 °C with 5% CO_2 for 3 h. Then each cell plate was washed twice with 200 μl per well of Rb^+-free DMEM/F12 medium and redispensed with DMEM/F12 medium containing 50 mM KCl. After incubation at 22 °C for 10 min, the supernatant was transferred to a new 96-well plate. The cells were then lysed with 200 μl per well of 1% Triton in phosphate-buffered saline. Rb^+ concentrations in both supernatant and cell lysates were measured by atomic absorption spectrometry using an ICR8000 instrument (Aurora Biomed).

Mutagenesis. Starting from KCNQ cDNAs, the KCNQ2 point mutants were constructed by recombinant PCR and verified by sequencing.

Modeling. Three-dimensional structural models for the KCNQ2 S5-S6 domains were generated using the solved crystal structure of Kv1.2 (Protein Data Bank code 2A79) as a template. The corresponding domains between KCNQ2 and Kv1.2 were aligned with DNASTAR MegAlign using standard parameters. The KCNQ2 models were constructed using DeepView/SWISS-PdbViewer (http://ca.expasy.org/spdbv)[55]. The structural representation was performed with PovRay (http://www.povray.org).

Neuron culture. Dorsal root ganglia (DRG) were collected from 14-d-old Sprague-Dawley (CD) rats and incubated in collagenase (Sigma, 500 U ml^{-1}, 15 min) and then trypsin (Sigma, 1 mg ml^{-1}, 30 min) at 37 °C. Single DRG neurons were isolated by mechanical trituration with a fire-polished glass Pasteur pipette. Hippocampal tissue was dissected out from CD rats on

postnatal day 0. The tissue was digested with papain (Worthington Biochem, 20 U ml^{-1}, 30 min) and resuspended into single cells. The single-cell suspension was plated onto a monolayer of glial cells that were growing on coated coverslips. Cytosine-1-D-arabinofuranoside at 5 μM was added into the culture medium 24 to 48 h later to arrest glial cell proliferation. The culture medium consisted of Neurobasal medium with B-27 supplement (Gibco), penicillin, streptomycin and 2 mM L-glutamine. All cells were maintained at 37 °C with 5% CO_2 before recording.

Electrophysiological recording. Standard whole-cell recording was used. Pipettes were pulled from borosilicate glass capillaries (TW150-4, World Precision Instruments). When filled with the intracellular solution, the pipettes have resistances of 3–5 MΩ. During the recording, constant perfusion of extracellular solution was maintained using a BPS perfusion system (ALA Scientific Instruments). Pipette solution contained (in mM): 145 KCl, 1 $MgCl_2$, 5 EGTA, 10 HEPES and 5 MgATP (pH 7.3); extracellular solution contained (in mM): 140 NaCl, 3 KCl, 2 $CaCl_2$, 1.5 $MgCl_2$, 10 HEPES and 10 glucose (pH 7.4). Current and voltage were recorded using an Axopatch-200A amplifier, filtered at 1 kHz, and digitized using a DigiData 1322A with pClamp 9.2 software (Axon Instruments). Series resistance compensation was also used and set to 60–80%.

For single-channel recording procedure, outside-out patch recording was used. The pipettes had resistances of 7–15 MΩ when filled with the intracellular solution of the following composition (in mM): 145 KCl, 1 $MgCl_2$, 5 EGTA, 10 HEPES and 5 MgATP (pH 7.3). Extracellular solution contained (in mM): 150 NaCl, 5 KCl, 2 $CaCl_2$, 1 $MgCl_2$, 10 HEPES and 10 glucose (pH 7.4). Current and voltage were recorded using an Axopatch-200B amplifier, sampled at 4 kHz and filtered at 200 Hz, and digitized using a DigiData 1322A with pClamp 9.2 software (Axon Instruments).

The P_o and single-channel current (i) were calculated by fitting all-point histograms with single- or multi-Gaussian curves. The ratio of the area under the fitted 'open' Gaussian to the total area under the entire Gaussian was taken as P_o, and the difference between the fitted 'closed' and 'open' peaks was taken as i. Single-channel conductance (γ) was calculated using the equation $\gamma = i/(V - V_E)$, where V is depolarized potential and V_E is reversal potential of potassium.

Data and statistical analysis. Patch-clamp data were preprocessed using Clampfit 9.2 (Axon Instruments) and then analyzed in Origin 7 (OriginLab). The activation curve was fitted by the Boltzmann equation: $G = (G_{max} - G_{min})/(1 + \exp[(V - V_{1/2})/S]) + G_{min}$, where G_{max} is the maximum conductance, G_{min} is the minimum conductance, $V_{1/2}$ is the voltage for half of the total number of channels to open and S is the slope factor. The dose-response curve was fitted by the Hill equation: $E = E_{max}/(1 + (EC_{50}/C)^P)$, where E_{max} is the maximum response, C is the drug concentration, EC_{50} is the drug concentration producing half of the maximum response, and P is the Hill coefficient. The deactivation trace was fitted by the standard exponential equation $I(t) = \Sigma I_i \times \exp(-t/\tau_i)$, where I is the current, t is the time and τ is the time constant. Data are presented as means ± s.e.m. Significance was estimated using the paired two-tailed Student's t-test.

Accession codes. Protein Data Bank: the crystal structure of Kv1.2 (deposited in a previous study) is listed as 2A79.

Note: Supplementary information and chemical compound information is available on the Nature Chemical Biology website.

ACKNOWLEDGMENTS

We thank T. Jentsch (Zentrum für Molekulare Neurobiologie, Hamburg), D. Makinnon (State University of New York, Stony Brook), M. Sanguinetti (University of Utah), M. Shapiro (University of Texas Health Science Center, San Antonio) and V. Vardanyan (Universität Hamburg) for gifts of cDNAs. We thank M. Fratine, A. Ince, S. Long, M. Spieker and K. Xie for technical assistance. We also thank B. Coblitz for help with structural modeling and our colleagues and members of the Li laboratory for valuable discussions and comments on the manuscript. The N-type calcium channel stable line was a kind gift from D. Lipscombe and D. Yue. This work is supported by a grant from the US National Institutes of Health to M.L. (GM70959).

AUTHOR CONTRIBUTIONS

Q.X. performed all electrophysiological recordings and analyses. H.S. performed high-throughput compound screens and constructed site-directed mutants. Q.X. and H.S. constructed vectors and established cell lines expressing KCNQ channels. M.L. helped conceive experiments.

COMPETING INTERESTS STATEMENT

The authors declare no competing financial interests.

Published online at http://www.nature.com/naturechemicalbiology
Reprints and permissions information is available online at http://npg.nature.com/reprintsandpermissions

1. Ashcroft, F.M. From molecule to malady. *Nature* **440**, 440–447 (2006).
2. Jan, L.Y. & Jan, Y.N. Cloned potassium channels from eukaryotes and prokaryotes. *Annu. Rev. Neurosci.* **20**, 91–123 (1997).
3. Tombola, F., Pathak, M.M. & Isacoff, E.Y. How far will you go to sense voltage? *Neuron* **48**, 719–725 (2005).
4. Brown, D.A. & Adams, P.R. Muscarinic suppression of a novel voltage-sensitive K+ current in a vertebrate neurone. *Nature* **283**, 673–676 (1980).
5. Marrion, N.V. Control of M-current. *Annu. Rev. Physiol.* **59**, 483–504 (1997).
6. Cooper, E.C., Harrington, E., Jan, Y.N. & Jan, L.Y. M channel KCNQ2 subunits are localized to key sites for control of neuronal network oscillations and synchronization in mouse brain. *J. Neurosci.* **21**, 9529–9540 (2001).
7. Schroeder, B.C., Kubisch, C., Stein, V. & Jentsch, T.J. Moderate loss of function of cyclic-AMP-modulated KCNQ2/KCNQ3 K+ channels causes epilepsy. *Nature* **396**, 687–690 (1998).
8. Hille, B. *Ion Channels of Excitable Membranes* 220–238 (Sinauer, Sunderland, Massachusetts, USA, 2001).
9. Jentsch, T.J. Neuronal KCNQ potassium channels: physiology and role in disease. *Nat. Rev. Neurosci.* **1**, 21–30 (2000).
10. Rogawski, M.A. KCNQ2/KCNQ3 K+ channels and the molecular pathogenesis of epilepsy: implications for therapy. *Trends Neurosci.* **23**, 393–398 (2000).
11. Charlier, C. *et al.* A pore mutation in a novel KQT-like potassium channel gene in an idiopathic epilepsy family. *Nat. Genet.* **18**, 53–55 (1998).
12. Gutman, G.A. *et al.* International Union of Pharmacology. XLI. Compendium of voltage-gated ion channels: potassium channels. *Pharmacol. Rev.* **55**, 583–586 (2003).
13. Kubisch, C. *et al.* KCNQ4, a novel potassium channel expressed in sensory outer hair cells, is mutated in dominant deafness. *Cell* **96**, 437–446 (1999).
14. Schroeder, B.C., Hechenberger, M., Weinreich, F., Kubisch, C. & Jentsch, T.J. KCNQ5, a novel potassium channel broadly expressed in brain, mediates M-type currents. *J. Biol. Chem.* **275**, 24089–24095 (2000).
15. Singh, N.A. *et al.* A novel potassium channel gene, KCNQ2, is mutated in an inherited epilepsy of newborns. *Nat. Genet.* **18**, 25–29 (1998).
16. Wang, Q. *et al.* Positional cloning of a novel potassium channel gene: KVLQT1 mutations cause cardiac arrhythmias. *Nat. Genet.* **12**, 17–23 (1996).
17. Shapiro, M.S. *et al.* Reconstitution of muscarinic modulation of the KCNQ2/KCNQ3 K(+) channels that underlie the neuronal M current. *J. Neurosci.* **20**, 1710–1721 (2000).
18. Wang, H.S. *et al.* KCNQ2 and KCNQ3 potassium channel subunits: molecular correlates of the M-channel. *Science* **282**, 1890–1893 (1998).
19. Cooper, E.C. & Jan, L.Y. Ion channel genes and human neurological disease: recent progress, prospects, and challenges. *Proc. Natl. Acad. Sci. USA* **96**, 4759–4766 (1999).
20. Armstrong, C.M. Time course of TEA(+)-induced anomalous rectification in squid giant axons. *J. Gen. Physiol.* **50**, 491–503 (1966).
21. Armstrong, C.M. Inactivation of the potassium conductance and related phenomena caused by quaternary ammonium ion injection in squid axons. *J. Gen. Physiol.* **54**, 553–575 (1969).
22. Armstrong, C.M. Interaction of tetraethylammonium ion derivatives with the potassium channels of giant axons. *J. Gen. Physiol.* **58**, 413–437 (1971).
23. Holmgren, M., Smith, P.L. & Yellen, G. Trapping of organic blockers by closing of voltage-dependent K+ channels: evidence for a trap door mechanism of activation gating. *J. Gen. Physiol.* **109**, 527–535 (1997).
24. Xu, J., Chen, Y. & Li, M. High-throughput technologies for studying potassium channels - progresses and challenges. *Targets* **3**, 32–38 (2004).
25. Sanguinetti, M.C. & Tristani-Firouzi, M. hERG potassium channels and cardiac arrhythmia. *Nature* **440**, 463–469 (2006).
26. Rostock, A. *et al.* D-23129: a new anticonvulsant with a broad spectrum activity in animal models of epileptic seizures. *Epilepsy Res.* **23**, 211–223 (1996).
27. Tober, C., Rostock, A., Rundfeldt, C. & Bartsch, R. D-23129: a potent anticonvulsant in the amygdala kindling model of complex partial seizures. *Eur. J. Pharmacol.* **303**, 163–169 (1996).
28. Rundfeldt, C. The new anticonvulsant retigabine (D-23129) acts as an opener of K+ channels in neuronal cells. *Eur. J. Pharmacol.* **336**, 243–249 (1997).
29. Tatulian, L., Delmas, P., Abogadie, F.C. & Brown, D.A. Activation of expressed KCNQ potassium currents and native neuronal M-type potassium currents by the anticonvulsant drug retigabine. *J. Neurosci.* **21**, 5535–5545 (2001).
30. Ramu, Y., Xu, Y. & Lu, Z. Enzymatic activation of voltage-gated potassium channels. *Nature* **442**, 696–699 (2006).
31. Sun, H., Shikano, S., Xiong, Q. & Li, M. Function recovery after chemobleaching (FRAC): evidence for activity silent membrane receptors on cell surface. *Proc. Natl. Acad. Sci. USA* **101**, 16964–16969 (2004).

32. Sun, H., Liu, X., Xiong, Q., Shikano, S. & Li, M. Chronic inhibition of cardiac kir2.1 and HERG potassium channels by celastrol with dual effects on both ion conductivity and protein trafficking. *J. Biol. Chem.* **281**, 5877–5884 (2006).
33. Terstappen, G.C. Functional analysis of native and recombinant ion channels using a high-capacity nonradioactive rubidium efflux assay. *Anal. Biochem.* **272**, 149–155 (1999).
34. Wickenden, A.D., Yu, W., Zou, A., Jegla, T. & Wagoner, P.K. Retigabine, a novel anti-convulsant, enhances activation of KCNQ2/Q3 potassium channels. *Mol. Pharmacol.* **58**, 591–600 (2000).
35. Bond, A.D.J. Synthesis and characterization of a novel zinc pyrithione hydrate. *Mol. Cryst. Liq. Cryst. Sci. Technol.* **356**, 305–313 (2001).
36. Wang, D.W. Synthesis of *N*-oxide-2-mercaptopyridine zinc salt. *Riyong Huaxue Gongye* **33**, 340–342 (2003).
37. Kimura, E., Takasawa, R., Tanuma, S. & Aoki, S. Monitoring apoptosis with fluorescent Zn^{2+}-indicators. *Sci. STKE* **2004**, PL7 (2004).
38. Barnett, B.L., Kretschmar, H.C. & Hartman, F.A. Structural characterization of bis(*N*-oxopyridine-2-thionato)zinc (II). *Inorg. Chem.* **16**, 1834–1838 (1977).
39. Main, M.J. *et al.* Modulation of KCNQ2/3 potassium channels by the novel anti-convulsant retigabine. *Mol. Pharmacol.* **58**, 253–262 (2000).
40. Schenzer, A. *et al.* Molecular determinants of KCNQ (Kv7) K+ channel sensitivity to the anticonvulsant retigabine. *J. Neurosci.* **25**, 5051–5060 (2005).
41. Wuttke, T.V., Seebohm, G., Bail, S., Maljevic, S. & Lerche, H. The new anticonvulsant retigabine favors voltage-dependent opening of the Kv7.2 (KCNQ2) channel by binding to its activation gate. *Mol. Pharmacol.* **67**, 1009–1017 (2005).
42. Long, S.B., Campbell, E.B. & Mackinnon, R. Voltage sensor of Kv1.2: structural basis of electromechanical coupling. *Science* **309**, 903–908 (2005).
43. Seebohm, G. *et al.* Differential roles of S6 domain hinges in the gating of KCNQ potassium channels. *Biophys. J.* **90**, 2235–2244 (2006).
44. Biervert, C. *et al.* A potassium channel mutation in neonatal human epilepsy. *Science* **279**, 403–406 (1998).
45. Dedek, K. *et al.* Myokymia and neonatal epilepsy caused by a mutation in the voltage sensor of the KCNQ2 K+ channel. *Proc. Natl. Acad. Sci. USA* **98**, 12272–12277 (2001).
46. Horrigan, F.T. & Aldrich, R.W. Coupling between voltage sensor activation, Ca2+ binding and channel opening in large conductance (BK) potassium channels. *J. Gen. Physiol.* **120**, 267–305 (2002).
47. Bandell, M. *et al.* High-throughput random mutagenesis screen reveals TRPM8 residues specifically required for activation by menthol. *Nat. Neurosci.* **9**, 493–500 (2006).
48. Li, Y., Gamper, N. & Shapiro, M.S. Single-channel analysis of KCNQ K+ channels reveals the mechanism of augmentation by a cysteine-modifying reagent. *J. Neurosci.* **24**, 5079–5090 (2004).
49. Huang, C.C., Lesburg, C.A., Kiefer, L.L., Fierke, C.A. & Christianson, D.W. Reversal of the hydrogen bond to zinc ligand histidine-119 dramatically diminishes catalysis and enhances metal equilibration kinetics in carbonic anhydrase II. *Biochemistry* **35**, 3439–3446 (1996).
50. Laine, M. *et al.* Atomic proximity between S4 segment and pore domain in Shaker potassium channels. *Neuron* **39**, 467–481 (2003).
51. Shealy, R.T., Murphy, A.D., Ramarathnam, R., Jakobsson, E. & Subramaniam, S. Sequence-function analysis of the K+-selective family of ion channels using a comprehensive alignment and the KcsA channel structure. *Biophys. J.* **84**, 2929–2942 (2003).
52. Marks, R., Pearse, A.D. & Walker, A.P. The effects of a shampoo containing zinc pyrithione on the control of dandruff. *Br. J. Dermatol.* **112**, 415–422 (1985).
53. Fliss, H. Zinc ionophores as therapeutic agents. US patent 6,495,538 (2002).
54. Mathie, A., Sutton, G.L., Clarke, C.E. & Veale, E.L. Zinc and copper: pharmacological probes and endogenous modulators of neuronal excitability. *Pharmacol. Ther.* **111**, 567–583 (2006).
55. Guex, N. & Peitsch, M.C. SWISS-MODEL and the Swiss-PdbViewer: an environment for comparative protein modeling. *Electrophoresis* **18**, 2714–2723 (1997).

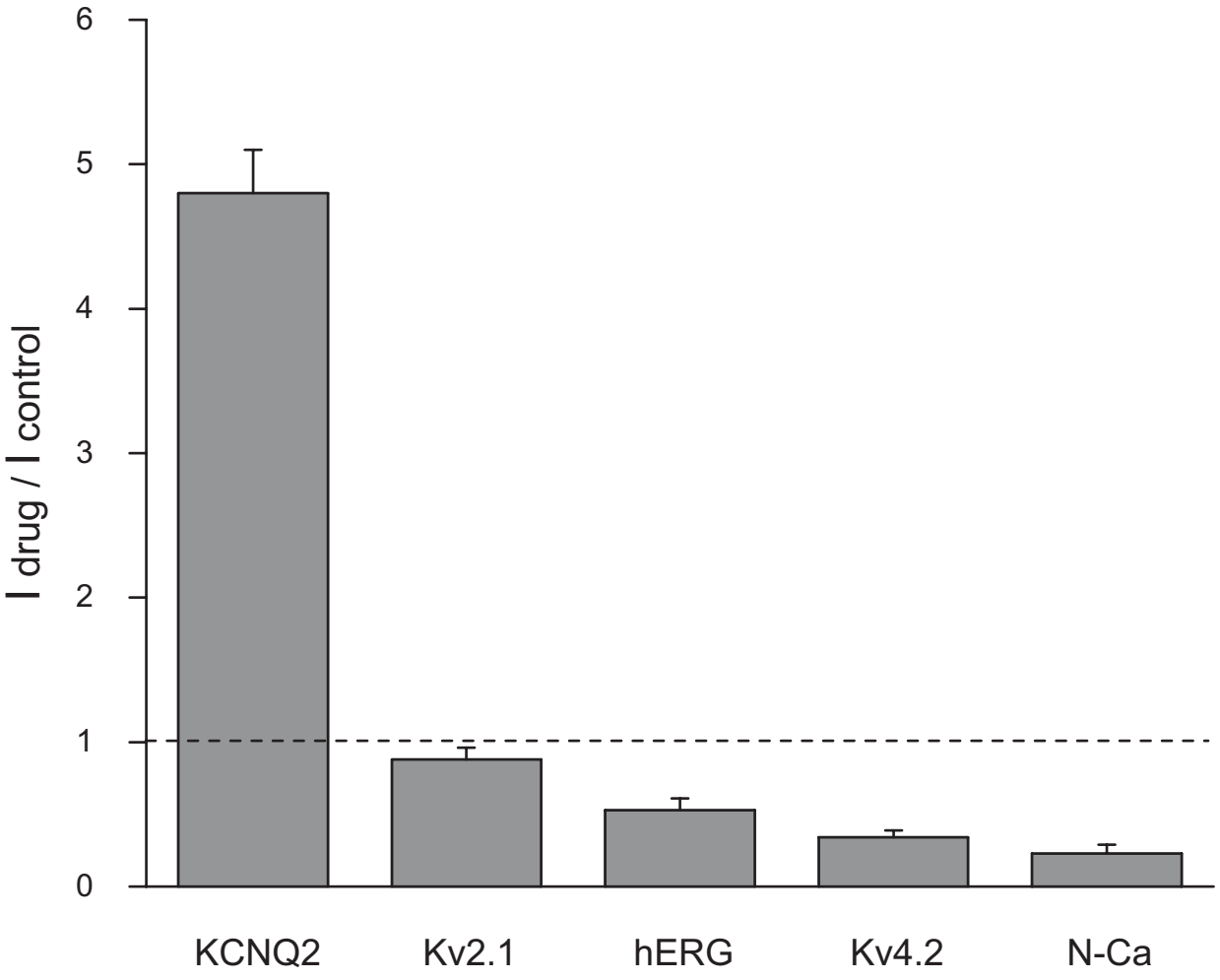

Figure S1. Zinc pyrithione effects on other potassium channels and N-type calcium channel. 10μM Zinc pyrithione were applied to each type of channel expressed in HEK293 cells. For different channels, currents were measured at different voltages: KCNQ2, +50 mV; Kv2.1, +10 mV; hERG, -50 mV; Kv4.2, +50 mV; N-Ca, 0 mV.

Figure S1 (Xiong et al., 2007)

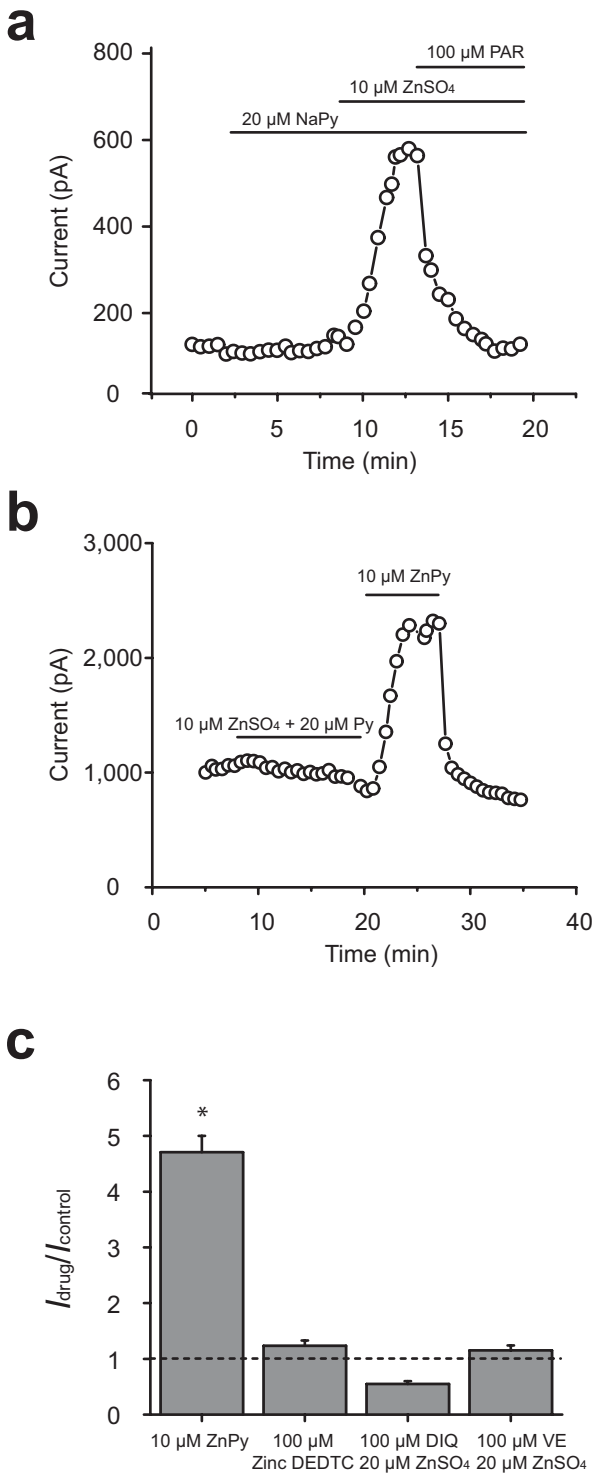

Figure S2. Complexed form of ZnPy is required for potentiation. a. Representative time course recordings of KCNQ2 current at +50 mV are shown. The overlapping time periods of external application of 20 μM sodium pyrithione (NaPy), 10 μM $ZnSO_4$, and 100 μM 4-(2)-(pyridylazo) resorcinol (PAR) are as shown. b. The non-overlapping time periods of external applications are shown. The first application is a mixture of 10 μM $ZnSO_4$ and 20 μM pyrithione (Py). The cell was then treated with 10 μM ZnPy upon the removal of the $ZnSO_4$ and pyrithione. c. Histogram summarizing the folds of potentiation at +50 mV by zinc ionophores including zinc diethyldithiocarbamate (DEDTC), 5,7-diiodo-8-hydroxyquinoline (DIQ) and (±)-α-tocopherol (VE) (n≥4, * p<0.001).

Figure S2 (Xiong et al., 2007)

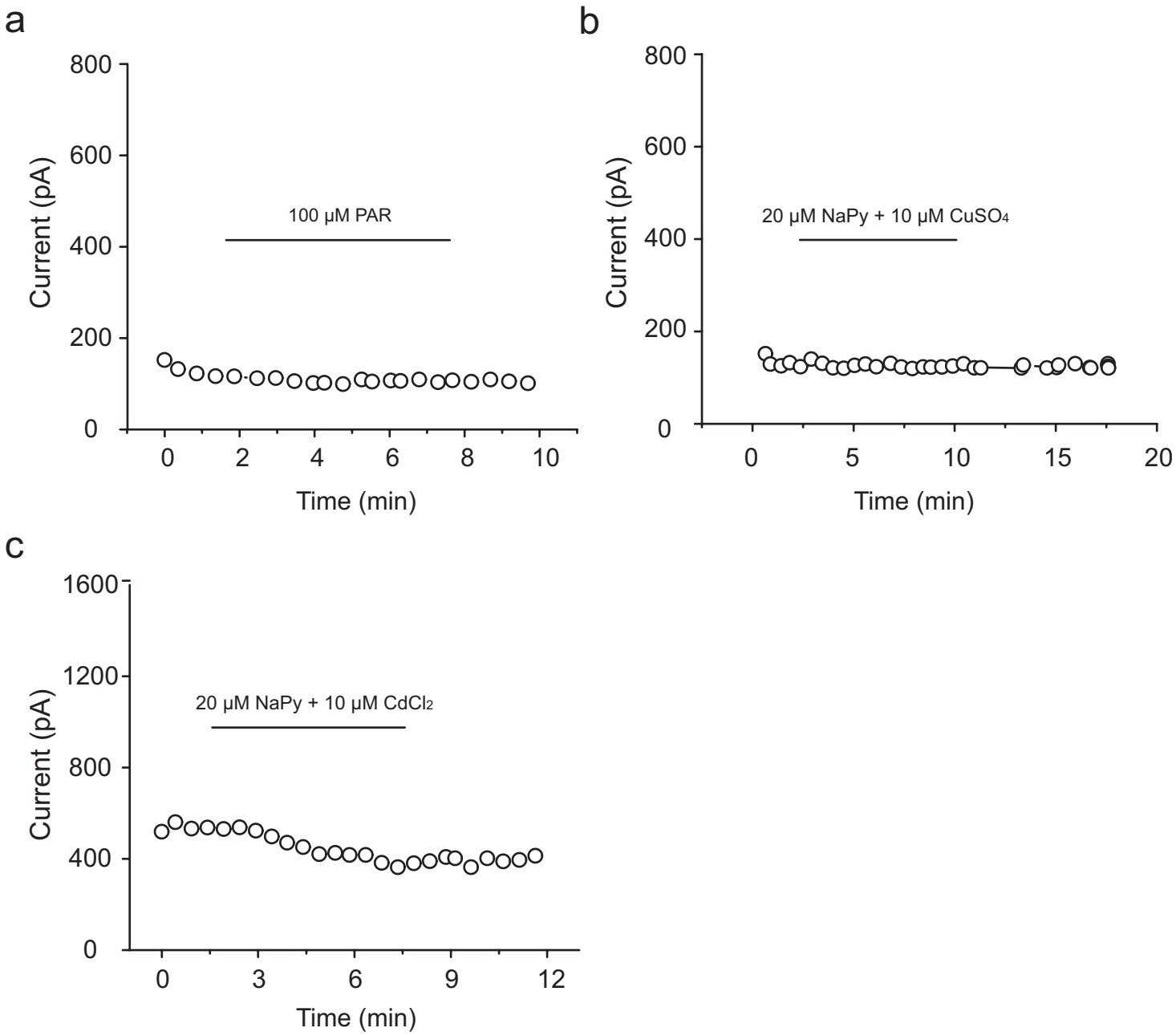

Figure S3. Other divalent ion effects on KCNQ2 current. a, Time course of KCNQ2 current at +50 mV when 100μM PAR was applied through bath solution (n=3, p>0.1). b, Time course of KCNQ2 current at +50 mV when the mixture of 20μM Na pyrithione and 10μM $CuSO_4$ was applied through bath solution (n=4, p>0.1). c, Time course of KCNQ2 current at +50 mV when the mixture of 20μM Na pyrithione and 10μM $CdCl_2$ was applied through bath solution (n=3, p>0.1).

Figure S3 (Xiong et al., 2007)

a

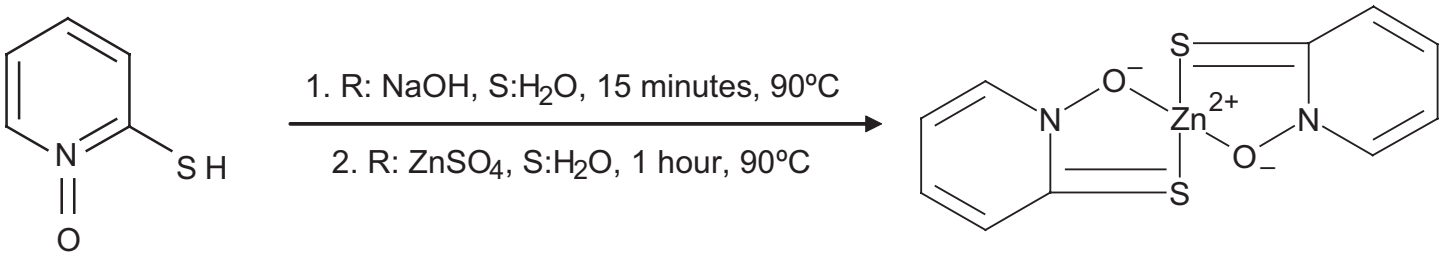

R: reactant, S: solvent

b

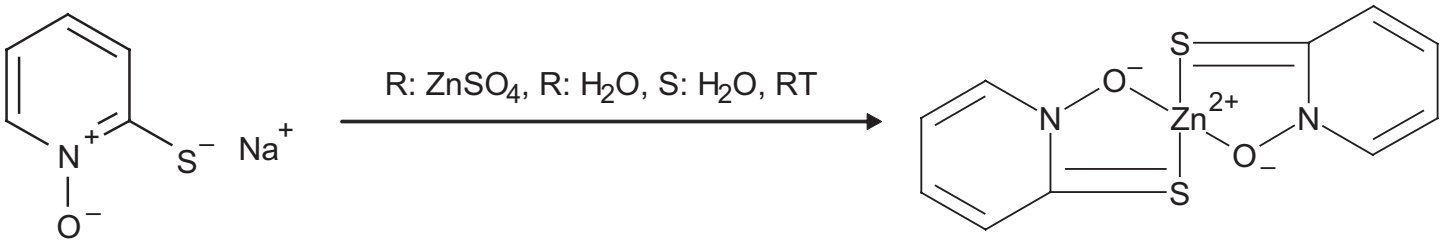

R: reactant, S: solvent, RT: room temperature

Figure S4. Synthesis of zinc pyrithione from pyrithione (a) or sodium pyrithione (b).

Figure S4 (Xiong et al., 2007)

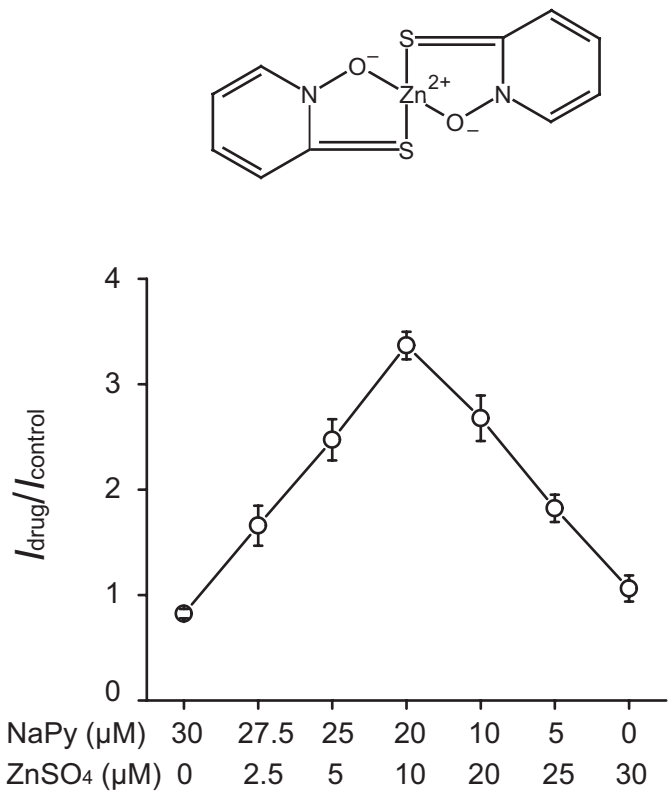

Figure S5. Stoichiometric preference of Zn ion and pyrithione. Structure of ZnPy is as shown according to the crystallographic studies. KCNQ2 current sensitivity was tested in the presence of mixtures of ZnSO4 and NaPy at the indicated ratios. KCNQ2 potentation is shown as normalized current obtained at +50 mV (n≥4).

Figure S5 (Xiong et al., 2007)

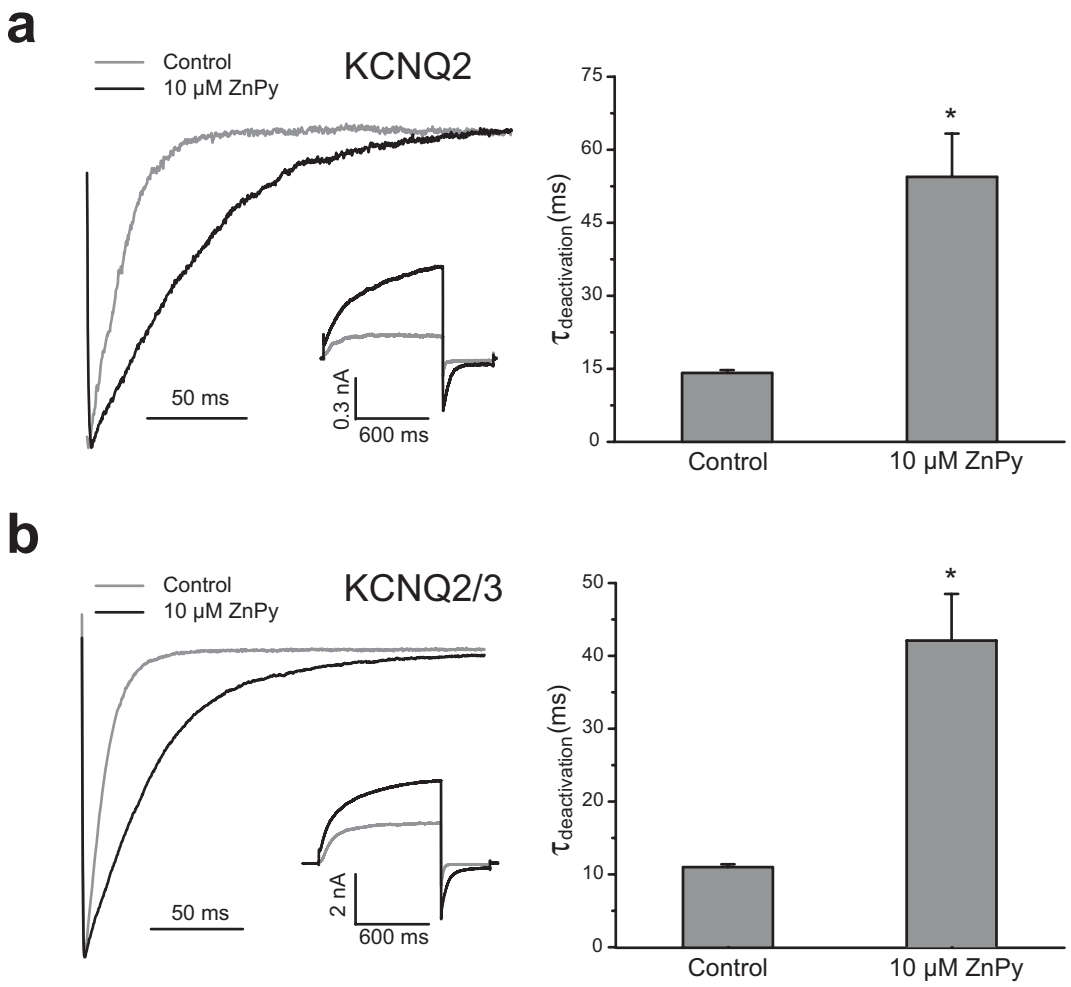

Figure S6. ZnPy effects on KCNQ2 and KCNQ2/3 deactivation. a and b, left panel shows the scaled tail currents from full traces (insert). Gray lines are the currents recorded in the control condition, and black lines are in the presence of 10 μM ZnPy. Vh was –80 mV, stepped to +50 mV, followed by -120 mV hyperpolarization. Right panel shows the deactivation time constants in the absence and presence of 10 μM ZnPy ($n \geq 4$, $p < 0.001$).

Figure S6 (Xiong et al., 2007)

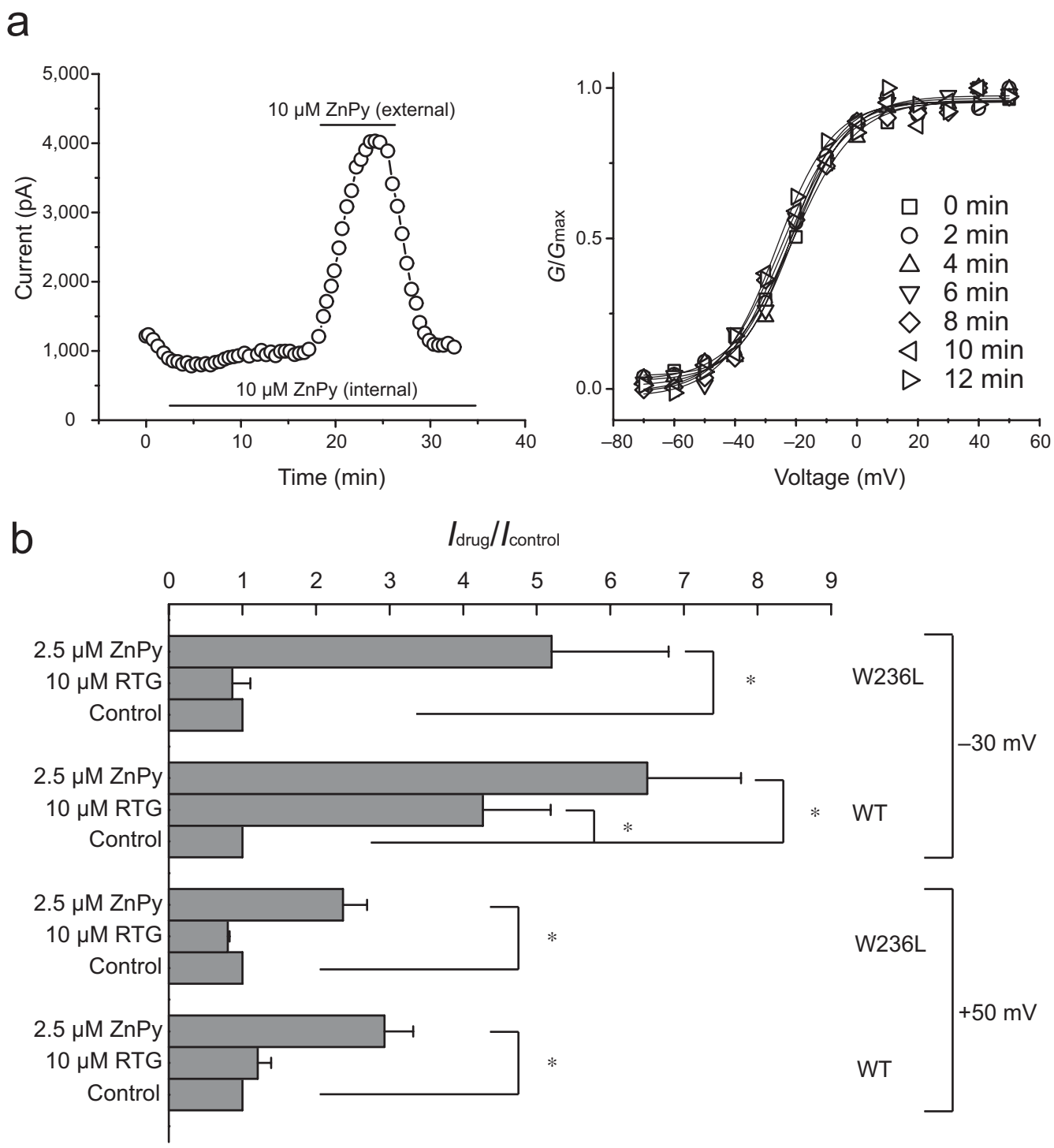

Figure S7. Differential modulatory sites on KCNQ channel by ZnPy and retigabine. a. Left Panel. Representative KCNQ2 current was recorded with intracellular pipet solution supplemented with 10 μM ZnPy. The overlapping external application of ZnPy is as shown. Right Panel. G-V curves at different indicated recording times (0 to 12 minutes) upon establishing stable seal are shown. The intracellular perfusion (with or without EGTA) was first calibrated by using compatible molecular weight dye. b. A histogram shows the comparison of ZnPy and retigabine (RTG) effects on KCNQ2 wild type and a KCNQ2 (W236L) mutant. 2.5 μM ZnPy or 10 μM RTG was applied separately to KCNQ2 wildtype (wt) or W236L. The levels of current potentiation at +50 mV and -30 mV were calculated by Idrug/Icontrol, and shown as indicated (n≥4, * p<0.001).